

ACKNOWLEDGEMENT



All praise due to Allah, the Most Gracious and the Most Merciful, for given me the strength, health and determination to complete my study project.

My utmost gratitude to my main supervisor, Dr. Ir. Bambang Basuno, for his sincere and frank advice constructive criticism and patient through out the study and during the preparation of this project. My great appreciation also goes to my second supervisor Dr. Zulkifly Abdullah for his precious and constructive criticisms that substantially improved this research.

The author would like to thank the Science University of Malaysia, who had given me the financial support to pursue my study.

My deepest gratitude and love to my parent who not only endured without any protest the loneliness while I prepared my thesis, but they also provided support, love and inspiration without which this research would have been never completed.

Finally, I thank all the staff and my friends at School of Aerospace Engineering, USM whom I cannot mention their names one by one, for the supports and criticisms for the further improvement of this research.

TABLE OF CONTENTS

	Page
ACKNOWLEDGEMENTS	ii
TABLE OF CONTENTS	iii
LIST OF TABLES	vi
LIST OF FIGURES	vii
NOMENCLATURE	xi
ABSTRAK	xiv
ABSTRACT	xv

CHAPTER ONE : INTRODUCTION

1.0	Introduction	1
1.1	Research Objective	4

CHAPTER TWO : LITERATURE REVIEW

1.0	Introduction	5
2.1	General Governing Equation	5
2.1.1	Navier-Stokes Equation	6
2.2	Inviscid flow: Potential flow	8
2.2.1	Panel method	9
2.2.2	Boundary condition of panel method	11
2.3	Viscous flow: Boundary layer	16
2.3.1	Conventional boundary layer formation	17
2.3.2	Separation	22
2.3.3	Boundary layer properties	23
2.4	Viscous-inviscid interaction	25
2.4.1	Coupling algorithm	26
2.4.2	Viscous-inviscid coupling technique	27
2.5	Implementation of viscous-inviscid on multi-element airfoil configuration	28

2.51 The multi-element airfoils boundary layer (flap configuration)	29
---	----

CHAPTER THREE: METHODOLOGY

3.0 Introduction	32
3.1 Potential flow: The mathematical approach	32
3.1.1 Lower order solution	34
3.1.2 Coordinate transformation	35
3.1.3 Incompressible velocity	37
3.1.4 Attached flow	40
3.1.5 Separated flow	44
3.1.6 Pressure coefficient	47
3.1.7 Multi-element system	48
3.2 Boundary layer: The mathematical approach	49
3.2.1 Thwaites's Method	51
3.2.2 Laminar-turbulent transition	55
3.2.3 Head's entrainment method	58

CHAPTER FOUR : COMPUTER CODE DEVELOPMENT

4.0 Introduction: Computational programming method	63
4.1 Computer code development	63
4.2 Description of the main subroutine	66
4.2.1 Main subroutine Airgm	66
4.2.2 Main subroutine Geom	66
4.2.3 Main subroutine Potfl	67
4.2.4 Main subroutine Bdylr	67
4.2.5 Main subroutine Loads	67
4.2.6 Main subroutine Plotres	68
4.3 Other subroutines	68
4.4 Functions	72

CHAPTER FIVE: RESULTS ANALYSIS AND DISCUSSION

5.0	Introductions	74
5.1	Aerodynamic analysis for single airfoil configuration	74
5.2	Results comparison	76
5.2.1	Results comparison between the inviscid flow and viscous-inviscid flow computation	76
5.2.2	Results comparison between the computational and experimental method	86
5.3	Detail of analysis on boundary layer solution	94
5.4	Aerodynamic analysis for multicomponent airfoil	103

CHAPTER SIX: CONCLUSION

6.0	Conclusion	123
6.1	Recommendation for further works	124

BIBLIOGRAPHY	126
---------------------	-----

APPENDICES

Appendix A :Table For Head and Patel Method

Appendix B: Computer program results listing for NACA 0012 at angle of attack, $\alpha=10$

Appendix C: Computer program results listing for NACA 4412 at angle of attack, $\alpha=10$

Appendix D: Computer program results listing for flapped GAW (1) at angle of attack, $\alpha=10$ and flap deflection angle, $\delta_f = 40^\circ$

Appendix E: MUFLOW sample results

LIST OF TABLES

	Description	Page
5.1	The position of transition point for NACA 0012 and NACA 4412 at $\alpha = 0^0, 5^0$ and 10^0	96
5.2a	Clean airfoil data geometry	104
5.2b	Clean airfoil data geometry (continue)	105
5.3a	Flap data geometry	105
5.3b	Flap data geometry (continue)	106

LIST OF FIGURES

	Description	Page
1.1	Comparison of results between experimental and panel method	3
2.1	Airfoil streamline with vortex and stagnation point on the airfoil's upper surface	14
2.2	Airfoil streamline with vortex and stagnation point on the airfoil's lower surface	14
2.3	Airfoil streamline with vortex and stagnation point at the trailing edge and cast off vortex	15
2.4	Boundary layer formation on the airfoil surface	18
2.5	Thickening of boundary layer on airfoil's surface	21
2.6	Displacement thickness description	24
2.7	Viscous-inviscid coupling technique	28
2.8	Boundary layer analysis on flap airfoil configuration	30
2.9	Merging of principle's airfoil wake with outer edge of the boundary layer on the flap's upper surface	31
3.1	Notation of velocity potential method	33
3.2	Discretization used in potential flow method	34
3.3a	Field point for coordinate transformation	35
3.3b	Control point for coordinate transformation	36
3.4	Notation for vortex and source distribution	38
3.5	Uniformly constant source	41
3.6	Piecewise constant source	42
3.7	Notation used in panel method modeling for separated flow	45
3.8	Augmented airfoil shape (outer flow model)	51

3.9	The stability curve	56
3.10	Transition curve	58
3.11	Control volume	59
4.1a	Computer code algorithm	64
4.1b	Computer code algorithm (continue)	65
5.1	NACA airfoil geometry	74
5.2	Pressure distribution comparison between inviscid and viscous-inviscid computation at zero degree angle of attack for NACA 0012	79
5.3	Pressure distribution comparison between inviscid and viscous-inviscid computation at five degree angle of attack for NACA 0012	80
5.4	Pressure distribution comparison between inviscid and viscous-inviscid computation at ten degree angle of attack for NACA 0012	81
5.5	Pressure distribution comparison between inviscid and viscous-inviscid computation at zero degree angle of attack for NACA 4412	82
5.6	Pressure distribution comparison between inviscid and viscous-inviscid computation at five degree angle of attack for NACA 4412	83
5.7	Pressure distribution comparison between inviscid and viscous-inviscid computation at ten degree angle of attack for NACA 4412	84
5.8	Graph of lift coefficient versus the number of iteration	86
5.9	Comparison of pressure distribution between experimental, computational and fully second order method on NACA 0012 at 2.84 Degree Angle of Attack	88
5.10	Comparison of pressure distribution between experimental, computational and fully second order method on NACA 0012 at 7.67 Degree Angle of Attack	89

5.11	Comparison of pressure distribution between computational and experimental on NACA 4412 at 1.2 Degree Angle of Attack	90
5.12	Graph of lift coefficient, C_l versus angle of attack, α for NACA 0012	92
5.13	Graph of lift coefficient, C_l versus angle of attack, α for NACA 4412	93
5.14	Displacement thicknesses for NACA 0012 at 0° , 5° and 10° angle of attack	97
5.15	Momentum thicknesses for NACA 0012 at 0° , 5° and 10° angle of attack	98
5.16	Shape Factor for NACA 0012 at 0° , 5° and 10° angle of attack	99
5.17	Displacement thicknesses for NACA 4412 at 0° , 5° and 10° angle of attack	100
5.18	Momentum thicknesses for NACA 4412 at 0° , 5° and 10° angle of attack	101
5.19	Shape Factor for NACA 4412 at 0° , 5° and 10° angle of attack	102
5.20	Pressure Distribution of Nested Flapped GAW (1) at 0° angle of attack	107
5.21	Pressure Distribution of Nested Flapped GAW (1) at 6° angle of attack	108
5.22	Pressure distribution on flapped GAW (1) ($\alpha = 0^\circ$, $\delta_f = 10^\circ$)	110
5.23	Pressure distribution on flapped GAW (1) ($\alpha = 0^\circ$, $\delta_f = 15^\circ$)	111
5.24	Pressure distribution on flapped GAW (1) ($\alpha = 0^\circ$, $\delta_f = 20^\circ$)	112
5.25	Pressure distribution on flapped GAW (1) ($\alpha = 0^\circ$, $\delta_f = 30^\circ$)	113
5.26	Pressure distribution on flapped GAW (1) ($\alpha = 0^\circ$, $\delta_f = 40^\circ$)	114
5.27	Pressure distribution on flapped GAW (1) ($\alpha = 5^\circ$, $\delta_f = 10^\circ$)	117

5.28	Pressure distribution on flapped GAW (1) ($\alpha = 15^0$, $\delta_f = 10^0$)	118
5.29	Pressure distribution on flapped GAW (1) ($\alpha = 5^0$, $\delta_f = 30^0$)	119
5.30	Pressure distribution on flapped GAW (1) ($\alpha = 10^0$, $\delta_f = 30^0$)	120
5.31	Pressure distribution on flapped GAW (1) ($\alpha = 5^0$, $\delta_f = 40^0$)	121
5.32	Pressure distribution on flapped GAW (1) ($\alpha = 10^0$, $\delta_f = 40^0$)	122

Nomenclature

C_d	Airfoil section drag coefficient
c_i	Length of i^{th} panel
C_f	Skin friction coefficient, $\frac{\tau_0}{q}$
C_l	Airfoil section lift coefficient
$C_{l,\max}$	Maximum section lift coefficient
C_{ref}	Reference chord
C_m	Airfoil section pitching moment coefficient with respect to 0.25C location
C_p	Coefficient of pressure
H_1	Head's mass flow shape factor
H_{12}	Boundary layer shape factor
H^*	Non-equilibrium value of H_1
I_1	Mass integral for an error function profile
I_2	Momentum integral for an error function profile
m	Streamline through $\phi = \frac{1}{2}(1 - \phi_B)(\eta = 0)$
M	Edge Mach number
M_∞	Freestream Mach number
n	Boundary layer exponent
P	Pressure

U	Edge velocity at the boundary layer, non-dimensionalized with respect to freestream velocity.
U_{∞}	Freestream velocity
u	Horizontal velocity in the global coordinate
u^n	Velocity component normal to a panel
u^t	Velocity component tangential to a panel
w	Vertical velocity in the global coordinate
Y_m	Coordinate shift between inviscid and intrinsic coordinate system

GREEK

α	Angle of attack
δ	Boundary layer thickness
δ_1	Displacement thickness
δ_2	Momentum thickness
δ_f	Flap deflection angle
ε	Apparent kinematics viscosity
η	Local coordinate normal to the panel or similarity variable
η_a	Upper trailing edge location
μ	Dynamic viscosity
ν	Kinematic viscosity
ξ	Local coordinate tangential to the panel
ρ	Density
τ	Wall shear stress

Φ Velocity potential

Subscripts

∞ Freestream condition

ANALISIS AERODINAMIK BERKOMPUTER TERHADAP KERAJANG UDARA MULTI-KOMPONEN DENGAN MENGGUNAKAN KAEDAH INTERAKSI LIKAT-TAK LIKAT

ABSTRAK

Kajian ini telah dijalankan berdasarkan pengaplikasian tentang interaksi aliran likat-tak likat. Sebuah program komputer telah dibina untuk mensimulasikan satu kaedah pasangan untuk aliran tak mampat subsonik berdua dimensi disekeliling konfigurasi satu dan kerajang udara multi-komponen. Kaedah berpasangan ini membawa maksud kepada perhubungan diantara kaedah panel 'linear vortex' dengan kaedah integrasi lapisan batas Von Karman. Teknik kaedah panel diaplikasikan untuk menghasilkan suatu nilai halaju bebas sebelum nilai tersebut dimasukkan ke dalam komputasi lapisan batas. Kaedah Thwaites adalah kaedah pertama yang digunakan untuk menyelesaikan masalah lapisan batas laminar sebelum kaedah Head mengambil alih tugas untuk pengiraan lapisan batas gelora. Lapisan batas telah menambah ketebalan efektif kerajang udara dengan satu nilai yang dinamakan sebagai ketebalan perubahan sebelum kaedah panel bertindak terhadap perubahan ini dengan cara menghitung semula nilai halaju bebas dan kemudian memasukan semula nilai halaju bebas yang baru ke dalam komputasi lapisan batas. Telah disimpulkan bahawa hanya empat iterasi yang diperlukan bagi menghasilkan jawapan yang menumpu. Validasi membuktikan komputasi terhadap kerajang udara NACA 0012, NACA 4412 dan GAW-1 ber'flap' berupaya menghasilkan jawapan yang menghampiri sembilan puluh peratus (90%) ketepatan apabila dibandingkan semula terhadap nilai-nilai dalam kaedah eksperimen. Walaubagaimanapun, kemampuan program komputer ini perlu dipertingkatkan memandangkan fenomena aliran terpisah masih belum lagi dilaksanakan.

COMPUTATIONAL AERODYNAMIC ANALYSIS OF MULTICOMPONENT AIRFOIL USING VISCOUS-INVISCID INTERACTION SCHEME

ABSTRACT

This research is accomplished based on the viscous-inviscid interaction appliance. A computer program is developed to simulate a coupling method for two-dimensional subsonic incompressible flow around single and multicomponent airfoil configurations. The coupling method signifies the interface linking both the linear vortex panel method and the Von Karman boundary layer integral. The panel method technique is applied in order to supply a freestream velocity value for the initial boundary layer computation. Concerning boundary layer computations, the Thwaites's method is initially used to determine the laminar boundary layer before the use of Head's entrainment method to verify the turbulent boundary layer. The boundary layer consequentially transforms the effective airfoil shape by the displacement thickness before the panel method reacts toward this altered effective shape by recalculating and circulating a new freestream velocity value into boundary layer solution. Validation demonstrates that the computation on NACA 0012, NACA 4412 and Airfoil with Flap (GAW-1 Airfoil) granted about ninety percent (90%) of conformity close to available experimental results in terms of pressure distributions, C_p and lift coefficient, C_l values. However, further enhancement for the developed computer code is necessary when in dealing with the flow separation phenomenon since its solution has not been implemented yet in the computer code.

Chapter 1: Introduction

1.0 Introduction

Physical flow phenomenon for air passing through a streamlined body shows that the viscous effect is limited to the flow region near the body surface. Such condition allows one to consider the flow around body to be divided into two main domains. They are known as:

1. The viscous flow region for the flow domain close to the body surface and
2. The inviscid flow domain for the flow domain relatively away from the surface of the body.

The first flow domain is sometimes called a boundary layer. The size of viscous flow domain depends on the type of flow, which developed into a particular region of laminar or turbulent flow. The Reynolds number of the flow under investigation will determine the thickness of the viscous flow region. If the flow is laminar, the thickness of viscous flow domain is in a magnitude order of $\frac{1}{\sqrt{R_L}}$, while during turbulent flow, a magnitude order

of $\frac{1}{\sqrt[5]{R_L}}$ is considered. Beyond those regions, one can consider that no viscous effect flow domain occurs. Naturally, the most aeronautical applications are related to flow problems with a high Reynolds number. It is because the viscous region is so thin and the flow domain is dominated by inviscid flow. In addition to that, for cases of flow passing through airfoil, wing, etc, problem solutions of the inviscid region could provide important and critical design informations. The inviscid problem solution could furnish knowledge on pressure distribution, which finally allows one to calculate lift and pitching moment coefficients. Subsequently, the inviscid solution may be used as a boundary condition for a

thin viscous boundary layer adjacent to the surface of body. This then permits one to obtain the boundary layer parameters such as skin friction, momentum and displacement thickness of a particular object under certain conditions.

The main part of this thesis is related to the analysis of the flow field, which will make use of a two-region flow model. One region has negligible viscous force while another region contains viscous force and is considered later.

The shearing stress can be expressed as the multiplication product of the viscosity μ and the shearing stress velocity gradient. There is no real fluid for which the viscosity is zero. However, there are many situations where the multiplication product of the viscosity and the shearing velocity gradient is sufficiently small, hence, ignoring shear stress terms when it is compared to other terms in the governing equations. When the term inviscid flow is used to describe the flow in those regions, the viscous shear stresses are negligibly small. By using the term of inviscid flow instead of inviscid fluid, emphasize is placed on assuming that the combined product of viscosity and the shearing velocity gradients have a small effect on the flow field and the fluid viscosity is assume to be zero. In fact, once the solution for the inviscid flow field is obtained, researchers may want to solve the boundary layer equations and calculate the skin friction drag on the configuration.

In the airfoil analysis, most of the model calculations were maybe conducted without considering the viscous effect on the airfoil. The result of the calculations are only mainly about the inviscid effect on the airfoil. However, the accuracy level of these models is significantly less since there are viscous effects, which undoubtedly gives a big impact on the airflow. Comparison between the experimental and theoretical results showed that

there is a slight difference in these two methods. This is because of the presence of viscous element in the experimental results.

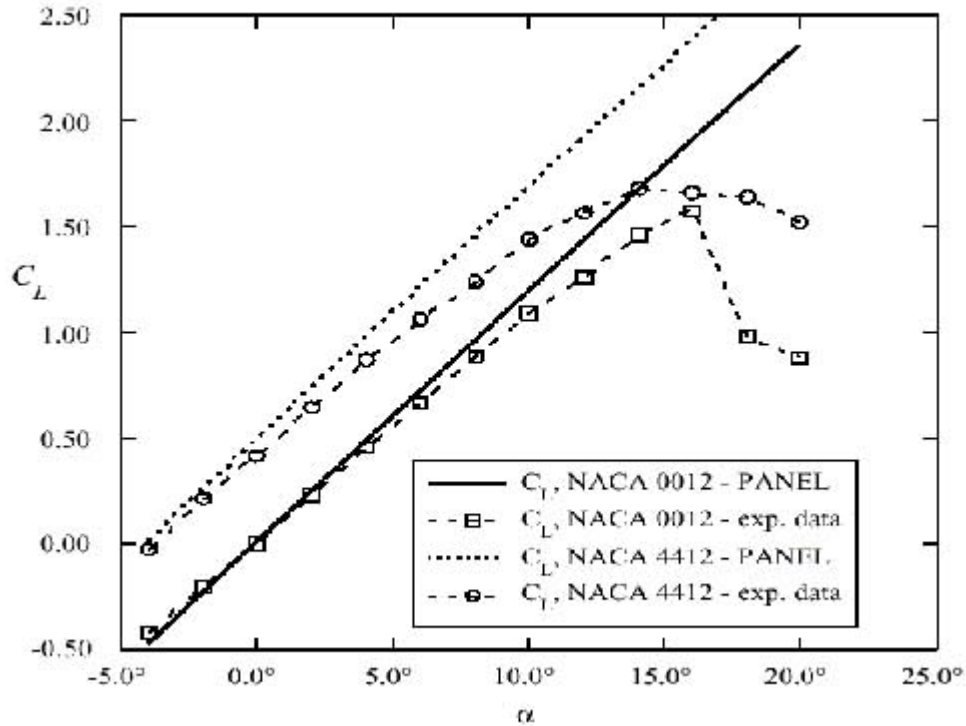


Figure 1.1. Comparison of results between experimental and panel method.
(Prabu et. al 2003)

The Figure 1.1 above shows the comparison result between panel method and experiment result for two types of NACA airfoil. The lift coefficient plotted with respect to the angle of attack. This graph shows that there is a slight difference between the experimental method and panel method. The experimental result illustrates that the lift coefficient change linearly until the angle of attack reached about 10 degrees. Here, one can find that the situation is different in the panel method results where the viscous effects were not taken into account. The panel method's result demonstrates that it maintains to be a linear increment at all angle of attack values. The maximum C_l value is at the highest angle of attack. As the results, there is no specified point of "stalling" angle of attack.

1.1. Research Objectives

The present research is done to develop a computer code for aerodynamics analysis, which is required in the aircraft design. Hopefully by the availability of this computer code it would make easier for any one in making assessment involving with single airfoil or multi component airfoil will be used in the aircraft design.

The main focus of this research is to develop a computer code that has capabilities for aerodynamics analysis purposes. The developed computer code would be able to do aerodynamics analysis whether the problem is single airfoil or multi component airfoils. The application of this computer code would be limited to the low subsonic flight since the governing equation of fluid motion that have been used in this present work is only to simulate the low subsonic flow model.

Chapter 2: Literature Review

2.0 Introduction

The governing equation of real airflow was already established nearly one and half centuries ago. This equation which is well known as The Navier Stokes allowed the capture of physical phenomenon which may appear in the real flow passing through a body. Unfortunately the exact solution of the Navier Stokes for the flow passing through an arbitrary body was not available. This chapter presents an overview to the approximate solutions of the Navier Stokes to the real airflow. The studies consist the Navier-Stokes capabilities either in the inviscid flow solver or the boundary layer solution. It also covers the coupling method of viscous-inviscid interaction. The scope of this review emphasizes on solving the flow on a single and multi-component airfoil configuration.

2.1 General governing equation

The governing equations of fluid dynamics represent the conservation of mass, momentum, and energy for a fluid continuum. The Governing Equations have actually been known for over 150 years. In the 19th century two scientists, Navier and Stokes described the equations for a viscous, compressible fluid, which are now known as the Navier-Stokes Equation (Nelson T.E. et. al, 1994). Considering a small or finite volume of fluid derives these equations. Though deceptively simple, only the emergence of ever-faster computers over the past two decades has made it possible to solve the real world problems governed by these equations (James A.F., 1994).

Despite their relatively old age, the Navier-Stokes (N-S) Equations have never been solved analytically. It is the numerical techniques used to solve these non-linear and coupled mathematical equations, which are commonly known as Computational Fluid

Dynamics, or better known as CFD in short. CFD is the only means of generating complete solutions at the present time. For a particular physical configuration, boundary conditions are defined which represents the friction, heat transfer, air flow etc (Anderson J., 2001). These are included as part of the source term over the past 25 years CFD techniques have been extensively and successfully applied in advanced technology, such as the nuclear and the aerospace industries.

2.1.1 Navier- Stokes equation

The ultimate mathematical statement of fluid dynamics, applicable across the spectrum of problem types, is the set of full Navier-Stokes equations (Currie I.G. et. al, 2002). Fundamentally these are capable of expressing any flow scenario, variety coming into the picture through different boundary conditions and auxiliary relations (Landau L. D. et al, 2000). However, the full equations are notoriously difficult to solve due to their non-linearity, their second-order form, and their multi-dimensional, etc (Kreiss H.O. et. al., 1989). Thankfully, flow analysts usually face situations where it is possible to simplify the equations and indeed it is part of their skill to recognize and exploit these opportunities. The governing equations of fluid dynamics in fact are from a hierarchy of increasing order of complexity and universality with the full Navier-Stokes equations on top.

From the full Navier-Stokes equations, with the consideration of turbulence by the Reynolds averaging and turbulence modeling, comes to another type of equation known as the Reynolds-averaged Navier-Stokes equation (Patrik R., 2001). This Reynolds-averaged Navier-Stokes equation relates to the classical view of turbulence as a time-average at a fixed point in space. The equations were derived in 1895 by Osborne Reynolds,

compromising each flow variable could be decomposed into a non-fluctuating, or mean, component plus a randomly fluctuating or turbulent component (Ockendon H et. al, 1995).

Moving to the next level of approximation, a deceptively simple notion provides the justification for viscous-inviscid interaction. This is the famous boundary-layer concept due to Prandtl in 1904 that assumes that at sufficiently high Reynolds numbers the effects of viscosity are confined to narrow layers adjacent to any solid boundaries. Conversely, outer region these 'boundary layers', the effects of viscosity are assumed negligible and thus there the flow is said to be inviscid (Schlichting, H. et. al, 2000). Consequently if one can consider such flow fields to be partitioned into two distinct zones, a boundary layer region where the effects of viscosity are concentrated, and a main flow or 'freestream' which is effectively inviscid. Viscous-inviscid interaction is a method of coupling the two regions. Separate calculations are performed for the two zones using separate sets of equations with the output from each providing boundary condition for the other. The process is repeated iteratively until convergence (Lock R.C. et. al., 1987).

Prandtl developed a reduced form of the governing equations for the boundary layer region known as the boundary-layer equations. Through an 'order of magnitude analysis', he retained only those terms of highest estimated magnitude or importance (for boundary layers) while everything of a lower order was dropped.

Another group of equation, sort of a compromise class of equations, simultaneously applicable to both viscous and inviscid flows but still not as complicated as the full Navier-Stokes equations, is the parabolized Navier-Stokes equations. These literally lie somewhere between the full Navier-Stokes and the boundary layer equations since this group of equations were derived from a similar order of magnitude analysis to Prandtl (Krause E., 2001). It has less restriction on the allowable magnitude of the terms retained. The

consequent elimination of the streamwise diffusion terms explains why this variant of the equations has a parabolic side to their nature.

As for the inviscid region, the equation hierarchy shows a sub-group of three types of equation the last of that is specific to aerodynamics. The least simplified and hence most generally applicable of the three are the Euler equations. These assume viscosity to be negligible with the consequence that the viscous terms in the momentum and energy equations are eliminated (Landau, L. D. et. al., 2000). Irrotationality tends to be the normal condition in the mainstream around a body immersed in an external flow (outside the shear layer at the body surface and the separated region or wake trailing downstream). With these considerations of irrotational flow in the Euler method, another type of equations called full potential equation produces. In this equation the body force terms is being dropped out and divergence form is used. The potential equation also includes the condition of uniform onset of flow where the shock is also considered to be in weak condition (Saad, M., 1998). Reducing down this full potential equation with the present of incompressible flow brings to the final equation for this inviscid region, which is called the Laplace's equation (Krantz, S. G., 1999).

2.2 Inviscid flow: Potential flow

Potential flow models have long been used in aerodynamics in a more or less sophisticated form. In the past decade the progress in computer technology has stimulated the use of the panel methods to an increasing scale of complexity.

For most of the methods currently in use the governing equation is based on Green's second identity, and is solved with the requirement of zero normal flow at the solid boundaries (Neumann boundary condition). In the meanwhile the formulation of the

inviscid problem has undergone very little refinement, whereas it was becoming evident that the step from the formulation to the numerical solution of the equations was not a simple solution. This step involves approximations of various sorts, among which two are easily identified (Brodkey R.S, 1995):

- The grid generation, the subdivision of the geometry into a number of elements of appropriate size and shape;
- The order of variation of the unknown over each element (low- or higher-order panel methods).

While most methods work, some work better with thick bodies (using Dirichlet boundary conditions), and others work better with thin bodies (using Neumann boundary conditions).

A Dirichlet boundary condition imposed on an ordinary differential equation or a partial differential equation where it specifies the values of a solution on the boundary of the domain. However in Neumann boundary condition cases, the partial differential equation only gives the normal derivatives values on the domain's boundary. Among the latter ones the velocity potential method is probably the most accurate (Emanuel G., 1994).

2.2.1 Panel methods

Panel methods offer a very elegant and powerful means of computation for flow past arbitrary bodies in two and three dimensions under various conditions of flow. The power of the method is both due to the fact that the differential equations are reduced to an integral form along the surface of the body and because the body in question is directly represented by a distribution of singularities on its surface. Hess and Smith (1967) laid the foundation for the source panel method. The idea of the vortex panel method is due to

Martensen (1971) and is extended by Lewis (1991). Katz and Plotkin (2001) gave a comprehensive overview of panel methods in general. In the following only two-dimensional, incompressible, inviscid flows are considered. There were no assumptions made on the geometry chosen. The basic philosophy being that one first splits the body geometrically into a set of panels and on the surface of each of these panels one distributes some kind of singularity distribution. Normally the body is reduced to a set of piecewise linear elements. Typically used singularity distributions are constant, linear and quadratic distributions of sources, vorticity and doublets. For a constant distribution of singularity, given a set of N panels this results in N unknowns. In order to solve for the singularity distribution one must specify N conditions to make the problem determinable. Once this is done, one solves a matrix to determine the unknown distribution of singularity. The conditions are applied at certain control points and can be specified in two ways, a velocity boundary condition (this is called the Neumann condition) and by the specification of the potential inside the body (the Dirichlet condition). The obvious disadvantage with the Dirichlet method is that one cannot solve for flow past thickness less bodies. However for closed bodies they produce very good results at low panel densities.

Yon (1990) performed an extensive study of nine different panel methods and reported finally that the combined constant source and doublet method with the Dirichlet formulation is the most robust from the practical requirements of speed and least sensitivity to panel densities. But for more complex geometries such as airfoils with cusped trailing edges or very thin airfoils, only the linear vortex Neumann formulation produced satisfactory results. This method was also found to be the only stable method that converged to the correct circulation around the lifting airfoils. Rajan (1994) also shows that a vorticity distribution on the surface of a body is capable of explaining the kinematics

motion of the rigid body in addition to solving the fluid flow. A distribution of doublets can also be used to solve the problem for lifting bodies; however, it can be easily shown that a polynomial distribution of doublets of order N can be reduced to a distribution of vorticity of order $N-1$. Due to the advantages of the linear vortex method and since the current work is interested in an accurate methodology for generalized bodies, both closed and open, thin and thick, and both lifting and non-lifting, a linear distribution of vorticity on the panels is chosen and the Neumann boundary condition (no penetration condition) is satisfied at the center of each panel.

2.2.2 Boundary conditions of panel method

There are a number of boundary conditions to be satisfied: a) boundary conditions on the body b) Kutta conditions at the trailing edge and c) conditions on the vortex wake (Katz J. et. al., 2001).

a) Boundary condition of the body

In a numerical procedure for body condition, depending on the formulation, either Dirichlet (thick body) or Neumann boundary (thin body) conditions are set. This inviscid flow solver provides the tangential velocity distribution on the airfoil's surface (U_∞). The pressure distribution is then computed from the velocity field using the Bernoulli equation. The lift and moment coefficients, as well as the pressure drag, are calculated by integrating the pressure over the body surface (Anderson, J, 2001). Velocity and pressure are dependent on each other. Bernoulli clearly stated that increasing the velocity decreases the local pressure and vice versa. Thus, the higher velocities on the upper airfoil side result in lower than ambient pressure whereas the pressure on the lower side is higher than the

ambient pressure. It is possible to plot a pressure distribution instead of the velocity distribution. Summing up the pressure acting on the airfoil results in a total pressure force. Splitting up this total pressure force into a part normal to the flow and another one tangential to the flow direction, results in a lift force L and a drag force D (Anderson J., 2001).

The magnitude of these aerodynamic forces depends on the combined effects of many different variables. The parameters that govern the magnitude of the aerodynamic forces and moments include (Bertin J. J. et. al., 1998):

- I. Airfoil geometry configuration
- II. Angle of attack
- III. Airfoil size or model scale
- IV. Freestream Velocity
- V. Density of the undisturbed air
- VI. Reynolds number
- VII. Mach number.

Since this research is done at constant Mach number, Reynolds number, free-stream velocity, size and at incompressible flows, the last five parameters are not being considered. Only the effects of airfoil geometry and angle of attack are the main criteria of evaluations.

i) Airfoil geometry parameters

There are four main airfoil geometry parameters that give the effect into the aerodynamic performances of an airfoil configuration, which are (Abbot I. et. al., 1959):

- 1) The leading edge radius
- 2) The mean chamber line

- 3) The maximum thickness and thickness distribution of the profile
- 4) Trailing edge angle

A different type of airfoil has their own parameters that give different results about the aerodynamic performances (Bertin J.J. et. al., 1998). There is wide range of airfoil configuration in the world today. However this scope of research concentrates on the NACA 0012, NACA 4412, GAW (1) and flapped GAW (1) configurations.

b) Kutta condition

Before analyzing the velocity and pressure field for the case of an airfoil, one needs to investigate the role played by circulation. The Kutta-Joukowski theorem shows that lift is proportional to circulation, but apparently the value of the circulation can be assigned arbitrarily. The solution of flow around an airfoil tells that one should expect to find two stagnation points along the airfoil the position of which is determined by the circulation around the profile. There is a particular value of the circulation that moves the rear stagnation point ($V=0$) exactly on the trailing edge. This condition, which fixes a value of the circulation by simple geometrical considerations, is known as the Kutta condition (McCormick W.B., 1995)

There are many different ways in which air is likely to circulate around the airfoil, depending on the pitch of the plane both vertically and horizontally. A variable airflow also affects lift or drag. Here, consideration is only about one shape of airfoil, which experience three separate types of uniform circulation. Figure 2.1 is a depiction of an airfoil undergoing a small circulation. The flow over the top is faster than the flow underneath, shown by the compact flow lines over the top edge



Figure 2.1 Airfoil streamline with vortex and stagnation point on the airfoil's upper surface

Although the top flow lines are close together, this circulation is not large enough to create the pressure imbalance needed to gain enough lift to get the plane lift off. This is observable in the flat flow lines on the underside of the wing; they are not rounded up towards the wing and do not produce much lift pressure. The topmost of the two flat flow lines experiences a small lift when the flow leaves the lower tip of the airfoil. This shows that the stagnation point of the airfoil have not moved down far enough for enough lift to occur; it is on the topside of this airfoil. Figure 2.2 shows the opposite effect

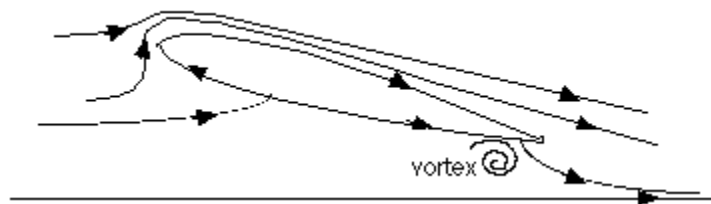


Figure 2.2. Airfoil streamline with vortex and stagnation point on the airfoil's lower surface

Here the air circulation is too large, creating a turbulent lift. One of the flow lines leaves the underside of the airfoil indicating not ideal conditions. The stagnation point in this case is too far down; it is on the underside of the airfoil. The lift provided by the circulation is enough to get the aircraft off the ground while at the same time providing a smooth rise. The Figure 2.3 reveals this condition

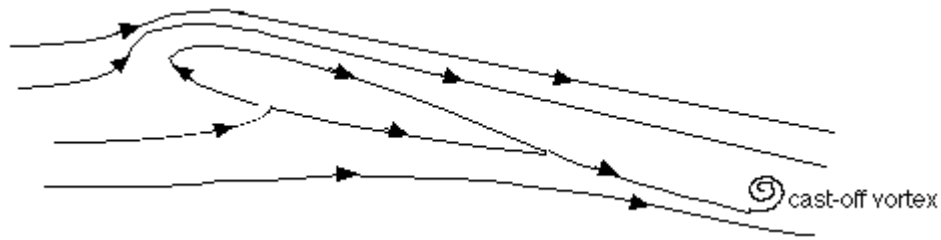


Figure 2.3. Airfoil streamline with stagnation point at the trailing edge and cast-off vortex

This condition seems to be ideal for planes lifting off. The stagnation point in this status is located at the trailing edge tip. This circulation provides a stable take off condition known as the Kutta Condition. The small vortexes shown in each Figure 2.1 to Figure 2.3 affect the lift or drag of the airfoil. In the Figure 2.1 the vortex is rotating counterclockwise and induces a downward flow on the wing. The circulation is thus affected and the stagnation points move downwards and rearward. The opposite effect takes place in the Figure 2.2. The vortex creates upwards flow on the underside of the wing, again moving the stagnation point's rearward. Each case is an undesirable result. The condition desired is shown in the Figure 2.3 with the airfoil in the Kutta condition (McCormick W.B., 1995). The vortex here is cast off well away behind the wing, making no interference with flight.

c) Boundary conditions on the wake

Consider a fluid particle flows within the boundary layer around the airfoil. From the pressure distribution measured in an earlier experiment, the pressure is a maximum at the stagnation point and gradually decreases along the front half of the airfoil. The flow stays attached in this favorable pressure region as expected. However, the pressure starts to increase in the rear half of the airfoil and the particle now experiences an adverse pressure

gradient. Consequently, the flow tends to separate from the surface and create a highly turbulent region behind the airfoil called the wake (McCormick W.B., 1995). The pressure inside the wake region remains low as the flow separates and a net pressure force (pressure drag) is produced.

2.3 Viscous flow: Boundary layer

The formulation and approximate solution of the boundary layer equations is historically the first entry in the array of the methods available in computational aerodynamics.

Back in the old days when calculations had to be done by hand, scientists used their intelligence to design practical methods. These methods are usually in integral form and provide global quantities relative to the viscous layers, namely displacement and momentum thickness, shape factor and higher order terms. These conditions are easy to set on flat plates aligned with the free stream, but pose a challenging difficulty on more general cases, when flow separation is involved (White F.M., 2003).

From a mathematical point of view, instead, the boundary layer equations are a classical singular-perturbation problem (Bott D.M et. al, 1998). The singular perturbation theory is very useful to analyze the order of magnitude of the viscous layers and other important quantities. Like in the old days most computational methods today mostly rely on integral equations. These equations are of the Von Karman Boundary Layer Integral (Ockendon H., et. al, 1995).

2.3.1 Conventional boundary layer formation

In the real flow, an airfoil moving through the air experiences a parasite drag force, which is usually divided into two components: frictional drag, and pressure drag. Frictional drag comes from friction between the air and the surfaces over which it is flowing. This friction is associated with the development of boundary layers, and it scales with Reynolds number (Hewitt et. al, 1989). Pressure drag comes from the eddying motions that are set up in the fluid by the passage of the body. Formally, both types of drag are due to viscosity, but the distinction is useful because the two types of drag are due to different flow phenomena (Murthy S.N et. al, 1997). Frictional drag is important for attached flows (that is, there is no separation), and it is related to the surface area exposed to the flow. Pressure drag is important for separated flows, and it is related to the cross-sectional area of the body (Tritton D. J., 1989).

Because of air viscosity, it will encounter resistance to flow over the airfoil surface. The viscous nature of flow reduces the local velocities on the surface and accounts for the drag of skin friction. The retardation of air particles due to viscosity is greatest immediately adjacent to the surface. The layer of air created over the surface, which shows a local retardation of airflow from the viscosity, is termed the ‘boundary layer’ (Ockendon H., et. al, 1995).

The boundary layer is a very thin layer of air flowing over a surface of an aircraft. The molecules directly touching the surface of the wing move are virtually motionless. Each layer of molecules within the boundary layer moves faster than the layer that is closer to the surface of the wing. At the top of the boundary layer, the molecules move at the same speed as the molecules outside the boundary layer. This speed is called the free-stream

velocity (Douglas J.F. et. al., 2001). The actual speed at which the molecules move depends upon the shape of the wing, the friction, the viscosity, or stickiness of the air, and its compressibility (the last two effects is not considered in this research).

Further, boundary layers may be either laminar (layered), or turbulent (disordered) as shown in the Figure 2.4. As the boundary layer moves toward the center of the airfoil, it begins to lose speed due to skin friction drag. At its transition point, the boundary layer changes from laminar, where the velocity changes uniformly as one move away from the airfoil's surface, to turbulent, where the velocity is characterized by unsteady (changing with time) swirling flows inside the boundary layer (Schlichting, H. et. al, 2000).

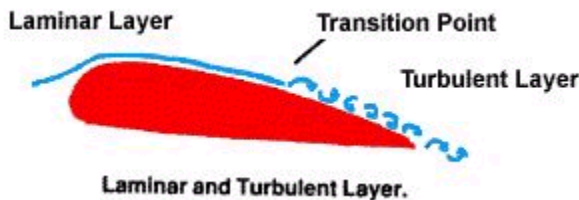


Figure 2.4. Boundary layer formation on airfoil surface (Allstar network FIU ,2002)

The flow outside of the boundary layer reacts to the shape of the edge of the boundary layer just as it would do to the physical surface of an airfoil. So the boundary layer gives the airfoil an "effective" shape that is usually slightly different from the physical shape (Young A.D, 1989). The boundary layer may also lift off or separate from the body, creating an effective shape much different from the physical shape of the airfoil and causing a dramatic decrease in lift and increase in drag. When this happens, the airfoil has stalled.

At small angles of attack, the laminar region on the top and bottom surface experience only mild pressure gradients and they remain attached along almost the entire chord length. Laminar creates only a thin region on the surface of the airfoil. The wake is very small, and the viscous friction inside the boundary layers dominates the drag. In this laminar region, the velocity profile is high which cause to the favorable pressure gradient (White F.M, 2003). Starting from the stagnation point at the leading edge, the laminar regions remains attach to the airfoil surface until the transition transforms the flow into turbulent boundary layer.

The onset of transition from the laminar boundary layer to a turbulent layer depends on many parameters such as the following (Bertin J.J et. al, 1998):

- Pressure gradient
- Surface roughness
- Compressibility effect
- Surface temperature
- Suction or blowing at the surface
- Free stream turbulence

In this research, only the discussion about pressure gradient will play an important role of determining the transition location.

The exact location of this transition point indicates the point, which separates the laminar and turbulent region. If this point is located at the rear of the airfoil, it means laminar region that has small frictional drag remains for a longer region and delays the pressure drag domination by the turbulent separation. This happens at small angle of attack. However, if the angle of attack is high, the transition point will moves its position towards

near the leading edge (Ockendon H., et. al, 1995). This means that the turbulent region remains a longer region than the laminar region. Turbulent boundary layer that has a larger frictional drag than the laminar tends to separate earlier since it has to go through a strong adverse pressure gradient at high angle of attack (Marusic et. al, 1995). This separation promotes early pressure drag domination on the airfoil surface as well.

Transition also plays an important role in determining the accuracy of the potential flow solution (Young A.D, 1989). This is because of its naturally separate the laminar boundary layer from the turbulent boundary layer. If the transition location delays at the trailing edge of an airfoil, it means that the laminar boundary layer dominates the surface of the airfoil. Consequently, the effective shape on the surface caused by the boundary layer is low since the thickness of boundary layer is thin. The potential flow solution is more accurate since the thin boundary layer gives a low “effective” shape (Young A.D, 1989). However, if the transition occurs early on the airfoil, the turbulence boundary layer dominates the airfoil and it caused a high “effective” shape (Young A.D, 1989). Thus, the turbulence boundary layer has a thicker boundary layer. This results in less accurate of potential flow solution.

Considering the flows on the airfoil where the transition has occurred and the boundary layer is fully turbulent, turbulent boundary layer is thicker than the laminar boundary layer (Schlichting, H. et. al, 2000). This thickening of boundary layer is shown in Figure 2.5. A turbulent flow is one in which irregular fluctuations (mixing or eddying motions) are superimposed on the mean flow. Thus, the velocity at any point in a turbulent boundary layer is a function of time. The fluctuations occur in the direction of the mean flow and at the right angles to it, and they affect in macroscopic lumps of the air (Bertin J.J et. al, 1998).

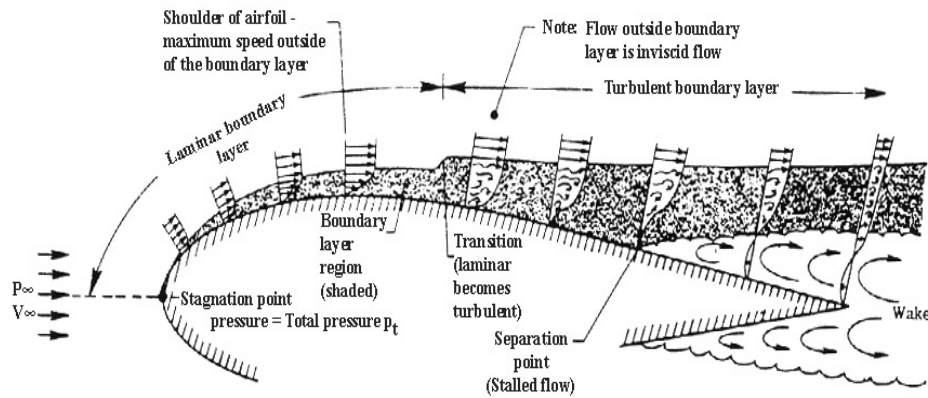


Figure 2.5. Thickening of boundary layer on airfoil's surface (www. centennialofflight.gov)

Therefore, even when the inviscid (mean) flow are two dimensional, a turbulent boundary layer will be three dimensional because of the three-dimensional character of the fluctuations. However, whereas momentum transports occurs on a microscopic (or molecular) scale in a laminar boundary layer, it occurs in macroscopic scale in the turbulent boundary layer. It should be noted that, although the velocity fluctuations maybe only several percent of the local streamwise value, they have a decisive effect on the overall motion. The size of these macroscopic lumps determines the scale of turbulence (Bertin J.J et. al, 1998).

The effects of the fluctuations are as the viscosity was multiplied by a factor of 10 or more (Bertin J.J et. al, 1998). As a result, the shear forces on the airfoil surface and the skin friction component of the drag are much larger when the boundary layer is turbulence (Tomkins, C. D., 1997). However, if the turbulence boundary layer can negotiate an adverse pressure gradient for a longer distance, boundary layer separation maybe delayed or even avoided altogether. Delaying the onset of separation reduces the pressure component of the drag (pressure drag) on the airfoil (Simpson R.L., 1989).

As the angle of attack increases, the adverse pressure gradients on the airfoil increase in magnitude (Bertin J.J et. al, 1998). The separation of turbulent boundary layer introduces early at a high angle of attack cases. This will perform wake on the airfoil and pressure drag starts to dominate. Due to this pressure drag domination; turbulence boundary layer is not the main component in the boundary layer anymore. It will leads to the larger distribution of drag component as well as the drag coefficient (Bertin J.J et. al, 1998).

In particular, the adverse pressure gradient on the top rear portion of the airfoil may become sufficiently strong to produce a separated flow. This separation will increase the size of the wake, and the pressure losses in the wake due to Eddy formation. Therefore the pressure drag increases. At a higher angle of attack, a large fraction of the flow over the top surface of the airfoil may be separated, and the airfoil is considerably stalled. At this stage, the pressure drag is much greater than the frictional drag (Hewitt et. al, 1989).

The amount of drag generated also depends on the size of the airfoil. Drag is an aerodynamic force and therefore depends on the pressure variation of the air around the airfoil as it moves through the air. The total aerodynamic force is equal to the pressure times the surface area around the airfoil; drag is the component of this force along the flight direction. Like the other aerodynamic force (lift) the drag is proportional to the area of the airfoil (John S. D, 2003)

2.3.2 Separation

The models proposed by Jacob (1969) and Steinbach (1974) and subsequently modified by Hanh et. al (1973) consist of adding a source distribution in the aft region of the airfoil to stimulate the separated wake. The main differences in all these models are in their method of finding the source distribution that satisfies the boundary conditions and of

choosing the location of the separation point. These models produce wakes, which extend to infinity downstream, contrary to experimental observations. Flow visualization experiments show that the wake closes at a distance downstream from the trailing edge (Zumwalt et. al. 1977).

The model developed by Zumwalt et. al (1977), Gross (1978), and Pfeiffer et. al. (1982) takes into account the flow mechanism inside the separated region, such as reverse flow, recompression, etc. this model produced excellent result for isolated airfoils (Zumwalt et. al, 1977), airfoil with spoiler (Pfeiffer et. al., 1982), and airfoil with aileron (Zumwalt et. al, 1982),.

2.3.3 Boundary layer properties

The boundary layer properties are used in describing the size and the shape of the boundary layer. The properties are the displacement thickness, momentum thickness, skin friction coefficient and also the shape factor (Schlichting, H. et. al, 2000).

The displacement thickness, δ_1 , is the distance a streamline just outside the boundary layer is displaced away from the wall compared to the inviscid solution. Another way to describe it is the distance the wall would have to be displaced to yield the same solution for flow outside the boundary layer as the boundary layer equations yield (Schlichting, H. et. al, 2000). Still another way to describe displacement thickness is in Figure 2.6. The displacement thickness is the distance that, when multiplied by the free-stream velocity, equals the integral of velocity defect, $U - u$ across the boundary layer. That is,

$$U\delta_1 = \int_0^{\infty} (U - u)dy \quad (2.5)$$

Solving for δ_1

$$\delta_1 \equiv \int_0^{\infty} \left(1 - \frac{u}{U}\right) dy \quad (2.6)$$

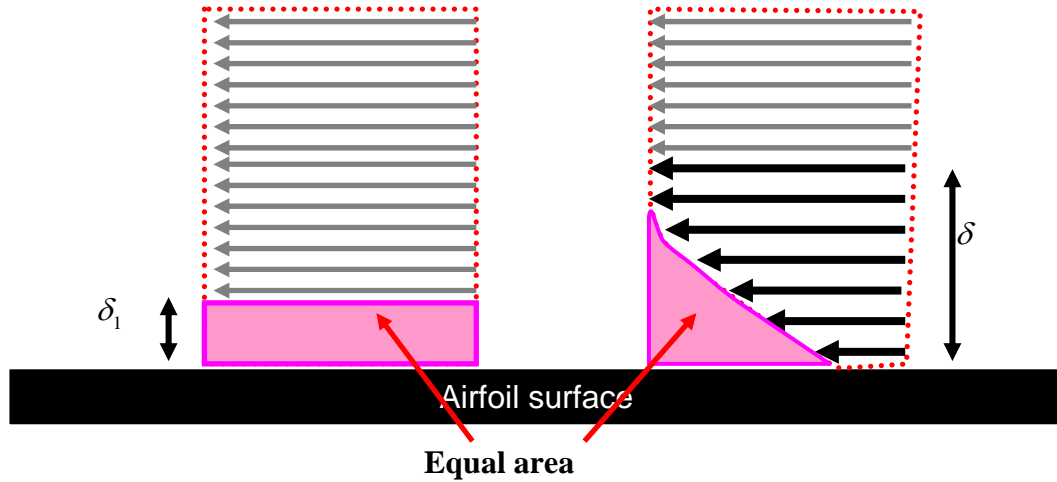


Figure 2.6. Displacement thickness description (Carl B.1999)

The displacement thickness is important in iterative boundary layer solutions. After employing the boundary layer equations to calculate the displacement thickness along the wall, a virtual wall is created by displacing the wall outward by the displacement thickness. A new inviscid solution is computed using this virtual wall. This yields slightly different free-stream conditions than the initial calculation. The boundary layer solution is then recalculated, using the new free-stream conditions, for the real wall. The process is repeated until the displacement thickness stops moving during iteration (Schlichting, H. et. al, 2000).

The second important character in the boundary layer sizing and shapes is the momentum thickness property, δ_2 . The concept is similar to that of displacement thickness in that δ_2 is related to the loss of momentum due to viscous effects in the boundary layer. Momentum thickness is the distance that when multiplied by the square of the free stream